

LARGE DEFORMATION HYPERELASTIC ANALYSIS IN MSC/NASTRAN Version 67.5

by

Katerina-D. P. Papoulia
Senior Development Engineer
The MacNeal Schwendler Corporation
Los Angeles, Ca.

and

Steve S. Hsieh
Manager
The MacNeal Schwendler Corporation
Hong Kong

ABSTRACT

Version 67.5 of MSC/NASTRAN includes finite deformation analysis for problems that involve large strain and large rotation. The material law is Green-elastic (hyperelastic) with a strain energy function of the generalized Rivlin type, extended to include the effect of compressibility at the nearly incompressible limit. The stress-strain relations are discussed in some detail as well as the approach taken to avoid the occurrence of volumetric locking. Examples are presented that illustrate the capabilities of the formulation to model problems with large strain and large rotation.

1. INTRODUCTION

Finite deformation analysis, which includes the effect of large rotation and large strain, is new to MSC/NASTRAN. The large rotation capability, provided with the PARAM,LGDISP,1 option for geometrically nonlinear analysis, assumes that the strains are infinitesimally small for all elements except those designated as FD (Finite Deformation). The approach for these fully nonlinear elements is total Lagrangian, as opposed to the corotational approach followed in geometric nonlinear analysis. A nonlinear strain measure is introduced, which is always measured from an initial undeformed state. Figure 1 illustrates the total Lagrangian concept in MSC/NASTRAN. The elements may be used in small strain situations and the results should be equivalent to those obtained from the corotational analysis for geometric nonlinearity only. However, the element library is not nearly as extensive: an 8-noded brick and a 4-noded plane strain quadrilateral are available. These seem to be adequate for the most part of nonlinear analysis that involves large strains.

The large strain capability is provided with one material option, namely hyperelasticity. This makes it applicable to materials undergoing large elastic deformations, such as elastomeric or rubber-like materials, used in the automobile and other industries. Examples are tires, O-rings, bushings, gaskets, seals and rubber boots. The most striking property of these materials, unfilled natural rubbers in particular, is their ability to withstand very large strains with very small deviation from elasticity. The stress-strain behavior of such materials is markedly nonlinear: A softening is generally observed with deformation, up to a certain level of straining, beyond which the material stiffens. The level of strain attained is typically of the order of several hundred percent.

The hyperelastic material in MSC/NASTRAN is specified on the MATHP bulk data entry and the fully nonlinear elements are activated by the PLPLANE and PLSOLID property entries.

2. THEORY

2.1. Stress-Strain Relations

Let \mathbf{x} and \mathbf{X} denote the current and original positions, respectively, of a material point and let

$$\mathbf{F} = \frac{\partial \mathbf{x}}{\partial \mathbf{X}} \quad (1)$$

be the deformation gradient, which fully describes the motion, including rigid body displacement and rotation. A hyperelastic or Green-elastic material is one for which a potential exists for the stresses in the form

$$\mathbf{S} = 2 \frac{\partial U(\mathbf{C})}{\partial \mathbf{C}} \quad (2)$$

where $U(\mathbf{C})$ is the elastic strain energy function, $\mathbf{C} = \mathbf{F}^T \mathbf{F}$ is the right Cauchy–Green tensor, measuring net deformation, excluding rigid body displacement and rotation, and \mathbf{S} is the symmetric (second) Piola–Kirchhoff stress, which is energetically conjugate to the Green–Lagrange strain $\mathbf{E} = (\mathbf{C} - \mathbf{1})/2$.

The theory of materials endowed with a strain energy function, which is a potential for the stresses, has been studied extensively and classical forms of this function due to Rivlin and Ogden [5] exist for incompressible materials. The assumption of incompressibility is, generally speaking, a reasonable one for rubber-like materials and has been used extensively as it considerably simplifies analytical solutions. In numerical solutions, however, it becomes a major difficulty, and a lot of research effort has been expended in either imposing the incompressibility constraint or addressing the problem of volumetric locking due to near-incompressibility. Extensions of the incompressible strain energy functions to include the effect of compressibility at the nearly-incompressible limit have been considered. To this end the decomposition

$$\bar{\mathbf{F}} = J^{-1/3} \mathbf{F} \quad (3)$$

is introduced, where $J = \det \mathbf{F}$ is a measure of volume change, $J = dV/dV_0$. This introduces a new motion $\bar{\mathbf{F}}$, which is volume preserving, since $\det \bar{\mathbf{F}} = J^{-1} \det \mathbf{F} = 1$, for which the incompressible strain energy function may be written in terms of the corresponding right Cauchy–Green tensor $\bar{\mathbf{C}} = \bar{\mathbf{F}}^T \bar{\mathbf{F}}$. In terms of these new variables the strain energy function becomes $\bar{U}(\bar{\mathbf{C}}, J) \equiv U(\mathbf{C})$, such that $\bar{U}(\bar{\mathbf{C}}, 1) \equiv U(\bar{\mathbf{C}})$. With the chain rule and standard results for the derivatives $\partial J / \partial \mathbf{C}$ and $\partial \bar{\mathbf{C}} / \partial \mathbf{C}$, the expression for the stress \mathbf{S} follows. For the present formulation in MSC/NASTRAN, however, the equations of motion will be written in the current (deformed) configuration¹ and therefore the Cauchy (true) stress $\sigma = (1/J) \mathbf{F} \mathbf{S} \mathbf{F}^T$ is the relevant measure of stress, which is

$$\sigma = \frac{\partial \bar{U}}{\partial J} \mathbf{1} + 2 \operatorname{dev} \left(\bar{\mathbf{F}} \frac{\partial \bar{U}}{\partial \bar{\mathbf{C}}} \bar{\mathbf{F}}^T \right) \quad (4)$$

and $\operatorname{dev}(\cdot) = (\cdot) - (1/3) \operatorname{tr}(\cdot) \mathbf{1}$. For isotropic materials, the dependence of the strain energy function on $\bar{\mathbf{C}}$ is through its invariants only. Such invariants are the eigenvalues $\bar{\lambda}_i^2$ of $\bar{\mathbf{C}}$ or the invariants \bar{I}_1, \bar{I}_2 defined below. Note that only two invariants are needed since $\bar{\lambda}_3 = \bar{\lambda}_1^{-1} \bar{\lambda}_2^{-1}$ and $\bar{I}_3 = \det \bar{\mathbf{C}} = 1$ due to the incompressibility of the motion $\bar{\mathbf{F}}$. The two classes of models are equivalent, since the invariants \bar{I}_1, \bar{I}_2 are symmetric functions of the principal stretches $\bar{\lambda}_p$. A particular form, separable in functions of $\bar{\lambda}_p$ is due to Ogden [5]. The

1. Some authors call this a total updated formulation [2].

strain energy function employed in MSC/NASTRAN is of the generalized Rivlin type and is of the form

$$\bar{U}(\bar{I}_1, \bar{I}_2, J) = \sum_{i,j \geq 0}^{N_A} A_{ij}(\bar{I}_1 - 3)^i(\bar{I}_2 - 3)^j + \sum_{i=1}^{N_D} D_i(J - 1)^{2i}, \quad A_{00} = 0 \quad (5)$$

where A_{ij} and D_i are material constants associated respectively with distortional and dilatational response. The Cauchy stress is given by

$$\sigma = p\mathbf{1} + \frac{2}{J} \text{dev} \left\{ \left(\frac{\partial \bar{U}}{\partial \bar{I}_1} + \bar{I}_1 \frac{\partial \bar{U}}{\partial \bar{I}_2} \right) \bar{\mathbf{B}} - \frac{\partial \bar{U}}{\partial \bar{I}_2} \bar{\mathbf{B}} \bar{\mathbf{B}} \right\} \quad (6)$$

where the pressure p is

$$p = \frac{\partial \bar{U}}{\partial J} \quad (7)$$

the invariants \bar{I}_1, \bar{I}_2 are

$$\begin{aligned} \bar{I}_1 &= \text{tr} \bar{\mathbf{B}} \\ \bar{I}_2 &= \frac{1}{2} [(\text{tr} \bar{\mathbf{B}})^2 - \bar{\mathbf{B}} : \bar{\mathbf{B}}] \end{aligned} \quad (8)$$

and

$$\bar{\mathbf{B}} = \bar{\mathbf{F}} \bar{\mathbf{F}}^T \quad (9)$$

is the left Cauchy–Green stretch tensor of the distortional deformation.

The model in MSC/NASTRAN assumes that distortional and volumetric deformations are uncoupled. A curve-fitting algorithm, based on least squares fitting, is available to determine the material constants A_{ij} and D_i , based on experimental data, up to the fifth order polynomial form. The constants D_i , associated with volumetric deformation, may be obtained from experimental data in pure volumetric compression, whereas the material constants A_{ij} , describing distortional deformation, may be obtained from force-deformation data in the following experiments:

1. Simple tension/compression
2. Equibiaxial tension
3. Simple shear
4. Pure shear

The model can have up to five constants D_i and up to 20 constants A_{ij} . In the limit of small strains, it reduces to a linear elastic material with the bulk and shear moduli respectively given by

$$\begin{aligned} K &= 2D_1 \\ G &= 2(A_{10} + A_{01}) \end{aligned} \quad (10)$$

A materially linear elastic analysis with the constants defined above (possibly including geometric nonlinearity) and a hyperelastic analysis of a small strain problem should give similar results. As seen from equation (5), the bulk modulus acts as a penalty in imposing the near-incompressibility constraint.

2.2. Volumetric Locking Avoidance

Typically, for rubbers, the bulk modulus is several orders of magnitude higher than the shear modulus. This introduces difficulties, which include ill-conditioning of the stiffness matrix, incorrect stresses, and 'locking' of the displacements [7]. As the nearly incompressible material approaches full incompressibility, the bulk modulus becomes infinite and the volumetric strain $J - 1$ becomes zero, so that the constitutive equation $p = \partial \bar{U} / \partial J$ predicts some finite but indefinite value for the pressure. The pressure may no longer be obtained from the displacements. It becomes an independent variable that may be calculated from the equilibrium equations and boundary conditions. In that spirit, the pressure and/or volume ratio are interpolated independently from the displacements in so-called mixed formulations, in which the following augmented energy functional is minimized to obtain the virtual work equation

$$\begin{aligned} \delta W^{int} + \delta W^{ext} &= 0 \\ \delta W^{int} &= \int_{B_0} \mathbf{S}^T \delta \mathbf{E} dV_0 = \int_B \sigma^T \nabla^s(\delta \mathbf{u}) dV \end{aligned} \quad (11)$$

plus additional equations for the mixed variables \hat{J}, \hat{p} :

$$W(\mathbf{u}, \hat{J}, \hat{p}) = \int_{B_0} [\bar{U}(\bar{I}_1, \bar{I}_2, \hat{J}) + \hat{p}(J - \hat{J})] dV_0 + W^{ext}(\mathbf{u}) \quad (12)$$

where B_0 and B are the initial and current volume of the body, respectively, and $\nabla^s(\delta \mathbf{u})$ is the symmetric gradient of the virtual displacement with respect to current coordinates. The invariants \bar{I}_1, \bar{I}_2 are functions of the displacements, while the volume ratio and the pressure are additional independent variables. Full Gaussian integration is used in evaluating the element integrals.

Alternatively a displacement formulation may be used with reduced integration of the volumetric terms in the force vector and in the stiffness matrix, which are given by the following expressions:

$$\mathbf{f}_I^e = \int_B (\mathbf{B}_I^{eT} \text{dev} \boldsymbol{\sigma} + \mathbf{B}_I^{vT} p) dV \quad (13)$$

$$\mathbf{K}_{IJ}^e = \int_B (\mathbf{B}_I^{eT} \mathbf{C}^s \mathbf{B}_J^e + \mathbf{B}_I^{vT} K \mathbf{B}_J^v + \mathbf{B}_I^T \mathbf{S}_1 \mathbf{B}_J^T - 2 \mathbf{B}_I^{sT} \mathbf{S}_2 \mathbf{B}_J^s) dV. \quad (14)$$

In these, \mathbf{C}^s and K are distortional and volumetric constitutive tangents, respectively, \mathbf{S}_1 and \mathbf{S}_2 are matrices containing Cauchy stresses and \mathbf{B}_I^e , \mathbf{B}_I^v , \mathbf{B}_I , \mathbf{B}_I^s are transformation matrices:

$$\nabla \mathbf{u} = \mathbf{B}_I \hat{\mathbf{u}}_I, \quad \nabla^s \mathbf{u} = \mathbf{B}_I^s \hat{\mathbf{u}}_I, \quad \text{tr} \nabla \mathbf{u} = \mathbf{B}_I^v \hat{\mathbf{u}}_I, \quad \text{dev} \nabla^s \mathbf{u} = \mathbf{B}_I^e \hat{\mathbf{u}}_I, \quad (15)$$

where $\nabla \mathbf{u} \equiv \partial \mathbf{u} / \partial \mathbf{x}$, $\nabla^s \mathbf{u} = \nabla \mathbf{u} + (\nabla \mathbf{u})^T$, $\hat{\mathbf{u}}_I$ are the displacements at node I , and summation is implied on I . Reduced integration is essentially equivalent to the mixed formulation, if the order of the pressure interpolation is the same as the number of integration (pressure) points for the volumetric terms [4].

Both formulations are available in MSC/NASTRAN for a 4-noded plane strain quadrilateral and an 8-noded brick element. They behave essentially the same, however, the mixed formulation may not converge as well as the selective reduced integration when combined with the BFGS updates, if the volumetric constitutive relation is highly nonlinear. The elements are linear with constant pressure interpolation or with single point integration of the volumetric terms. In the notation of Sussman and Bathe [7] they are 4/1 and 8/1 elements.

3. EXAMPLES

3.1 Estimation of Material Parameters

Experimental data for natural rubber, obtained by Treloar [8] in simple tension, equibiaxial tension, and pure shear have been used to evaluate the material constants. A total of 20 experimental points was provided for estimation of the distortional parameters A_{ij} for first, second, and third order strain energy polynomial, with two, five, and nine material constants respectively. The two parameter model corresponds to the Mooney–Rivlin strain energy function. The curve-fitting algorithm in MSC/NASTRAN will fit the analytical closed-form solutions of the above test cases to the experimental data provided. It is based on the method of singular value decomposition, which provides a least squares solution even in the rank deficient case. Of all possible solutions this is the vector \mathbf{A} of coefficients A_{ij} possessing minimal length. A message will be issued to warn the user that the parameters obtained are not unique. Rank deficiency may occur if an insufficient number of experimental points is provided for a given order of strain energy polynomial. A non-unique solution will always be obtained if the parameters are fitted from pure or simple shear experiments only. For adequate representation of the material in multiaxial states of deformation,

it is recommended that at least an axial and a shear test be performed. Figure 2 shows MSC/NAS-TRAN results with the parameters obtained from the curve-fitting algorithm. As shown in the figure, exact agreement is found between the theoretical (used in parameter estimation) and the numerical solution for the three states of stress considered.

3.2 Stretching of a Rubber Rectangular Bar

A plane strain rubber rectangular bar is partially constrained at one end and is stretched at the opposite end. The free portion of the partially constrained end simulates the existence of a crack. The material is assumed to be of the Neo-Hookean type (i.e. Mooney-Rivlin with $A_{01} = 0$) with $A_{10} = 100$ psi and D_1 is set to 5×10^5 psi to simulate the nearly incompressible condition. The finite element model contains 182 finite deformation QUAD4 elements. The final configuration of the bar is shown in Figure 3. The shape of the deformed mesh agrees with the results reported in [6].

3.3 Rubber Bushing Problem

The cross sector of a rubber bushing is shown on Figure 4. It is assumed that the frame and internal shaft are rigid and rubber is perfectly bonded to these components. A Mooney-Rivlin material model is assumed with $A_{10} = 0.177N/mm^2$, $A_{01} = 0.045N/mm^2$ and $D_1 = 333N/mm^2$. The goal of the analysis is to determine the force-displacement curve of the unit. Considering symmetric conditions, only one-half of the rubber part was modeled with 72 finite deformation QUAD4 elements. The grid points on the outer boundary were fully constrained to simulate the rubber-frame interface. As for the grid points on the inner boundary, only the horizontal degrees of freedom were constrained, while the vertical degrees of freedom were tied together with MPC's. Force was applied to the top grid point on the inner wall in the vertical direction. The same problem was also tested using a 3-D model, which contains 72 finite deformation HEXA8 elements. The force-displacement curve obtained agrees with that reported in [7] for the same type elements. However, for a force P greater than approximately 200N this is an overly stiff solution. As reported in [7], the actual response of the bushing is almost linear and is close to that obtained from a linear solution, which predicts a stiffness $K = 135G$, where G is the shear modulus. There is no provision against shear locking in the finite deformation elements in version 67.5. For this reason, the elements are not appropriate for problems with dominant bending type deformation. Mesh refinement will help alleviate this problem. Due to severe mesh distortion, the full Newton method (ITER, 1) became difficult to converge for values of P greater than 400N. The force was successfully increased up to 800N when using the BFGS updates.

3.4 Lateral Compression of a Rubber Cylinder

An infinitely long rubber cylinder with a diameter of 0.4m was pressed laterally between two rigid plates. Due to symmetry, only the right lower quarter was modeled using 48 finite deformation QUAD4 plane strain elements. Material constants were set to $A_{10} = 0.293MPa$, $A_{01} = 0.177MPa$ and $D_1 = 705MPa$. The contact region was simulated both with gap elements

and with the new slideline contact capability of MSC/NASTRAN. A 3-D model using 48 finite deformation HEXA8 elements was also tested. The force-deformation curve obtained compares well with that obtained in [7], which in turn compares with the analytical solution due to Lindley. See [7] for a discussion of the Lindley and Hertz solutions.

4. CONCLUSIONS

The new fully nonlinear finite deformation elements in MSC/NASTRAN are capable of representing large rotation as well as large elastic deformation up to several hundred percent strain. The elements possess successful mechanisms for avoidance of volumetric locking and can therefore be used for the description of nearly incompressible rubber-like materials. Material response is described by a generalized Rivlin model, capable of representing highly nonlinear behavior in multiaxial states of deformation. A robust algorithm is provided for estimation of material parameters from experimental data. The elements are restricted to plane strain or three dimensional problems and are not recommended for use in situations where bending dominates.

ACKNOWLEDGEMENT/DEDICATION

Tim Bock was the software developer for this MSC/NASTRAN project. His contributions to the project were many. This paper is dedicated to Tim Bock's memory.

REFERENCES

1. MSC/NASTRAN Release Notes for Version 67.5.
2. Crisfield, M.A., *Non-linear Finite Element Analysis of Solids and Structures*, Vol. 1, John Wiley, 1991.
3. De Borst, R. and Van Den Bogert, P.A.J., "Modelling and Analysis of Rubberlike Materials", *Heron*, **33**, no. 1, 1988.
4. Malkus, D.S. and Hughes, T.J.R., "Mixed Finite Element Methods-Reduced and Selective Integration Techniques: A Unification of Concepts", *CMAME*, **15**, 63-81, 1978.
5. Ogden, R.W., "Elastic Deformations of Rubberlike Solids", *Mechanics of Solids*, The Rodney Hill 60th Anniversary Volume, Hopkins, H.G. and Sewell, M.J., editors, Pergamon Press, 1982.
6. Simo, J.C. and Taylor, R.L., "Quasi-incompressible Finite Elasticity in Principal Stretches. Continuum Basis and Numerical Algorithms", *CMAME*, **85**, 273-310, 1991.
7. Sussman, T. and Bathe, K.-J., "A Finite Element Formulation for Nonlinear Incompressible Elastic and Inelastic Analysis", *Computers and Structures*, **26**, no. 1/2, 357-409, 1987.
8. Treloar, L.R.G., "Stress-Strain Data for Vulcanized Rubber Under Various Types of Deformation", *Trans. Faraday Soc.* **40**, 59-70, 1944.

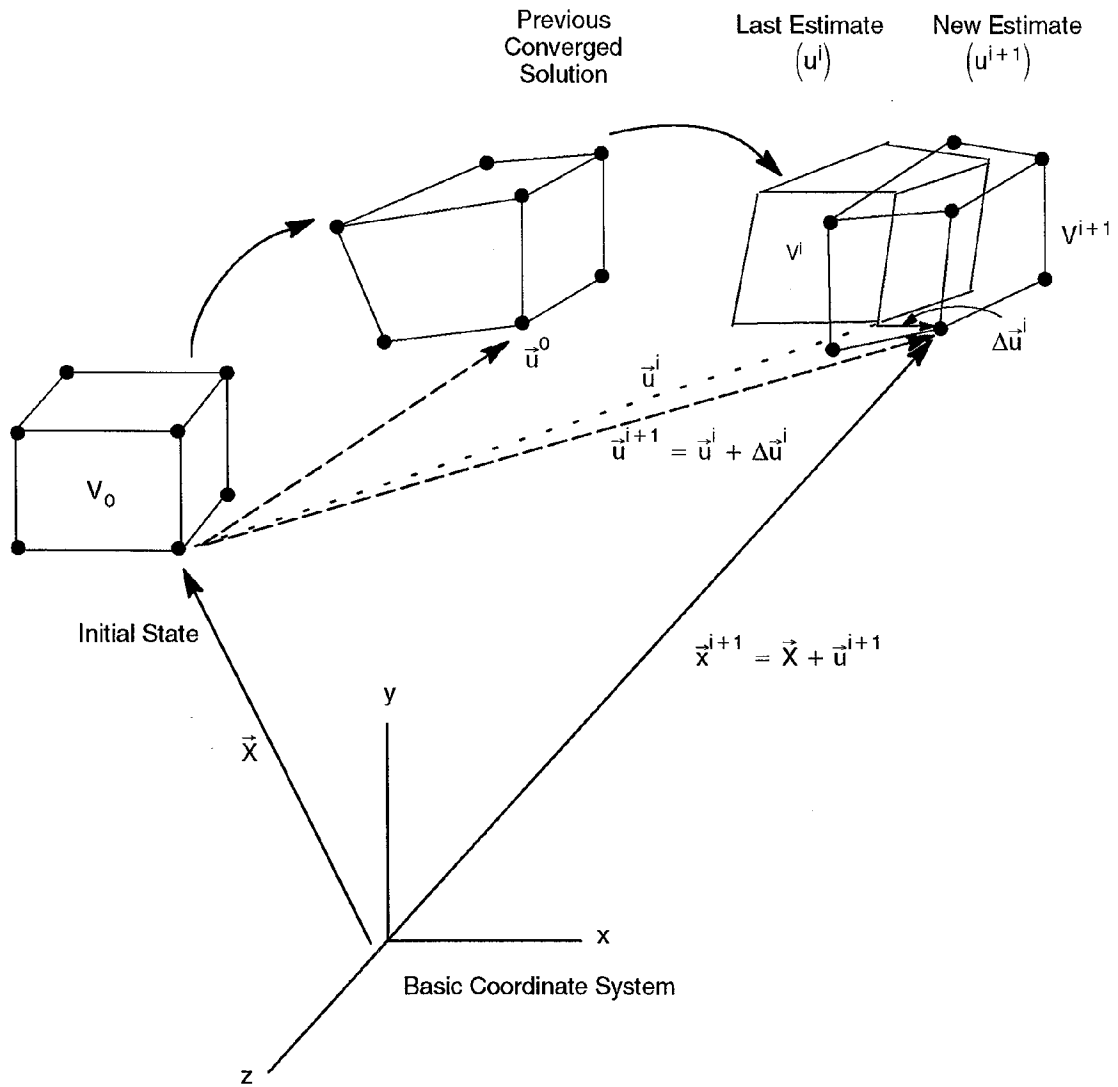


Figure 1. Total Lagrangian Formulation.

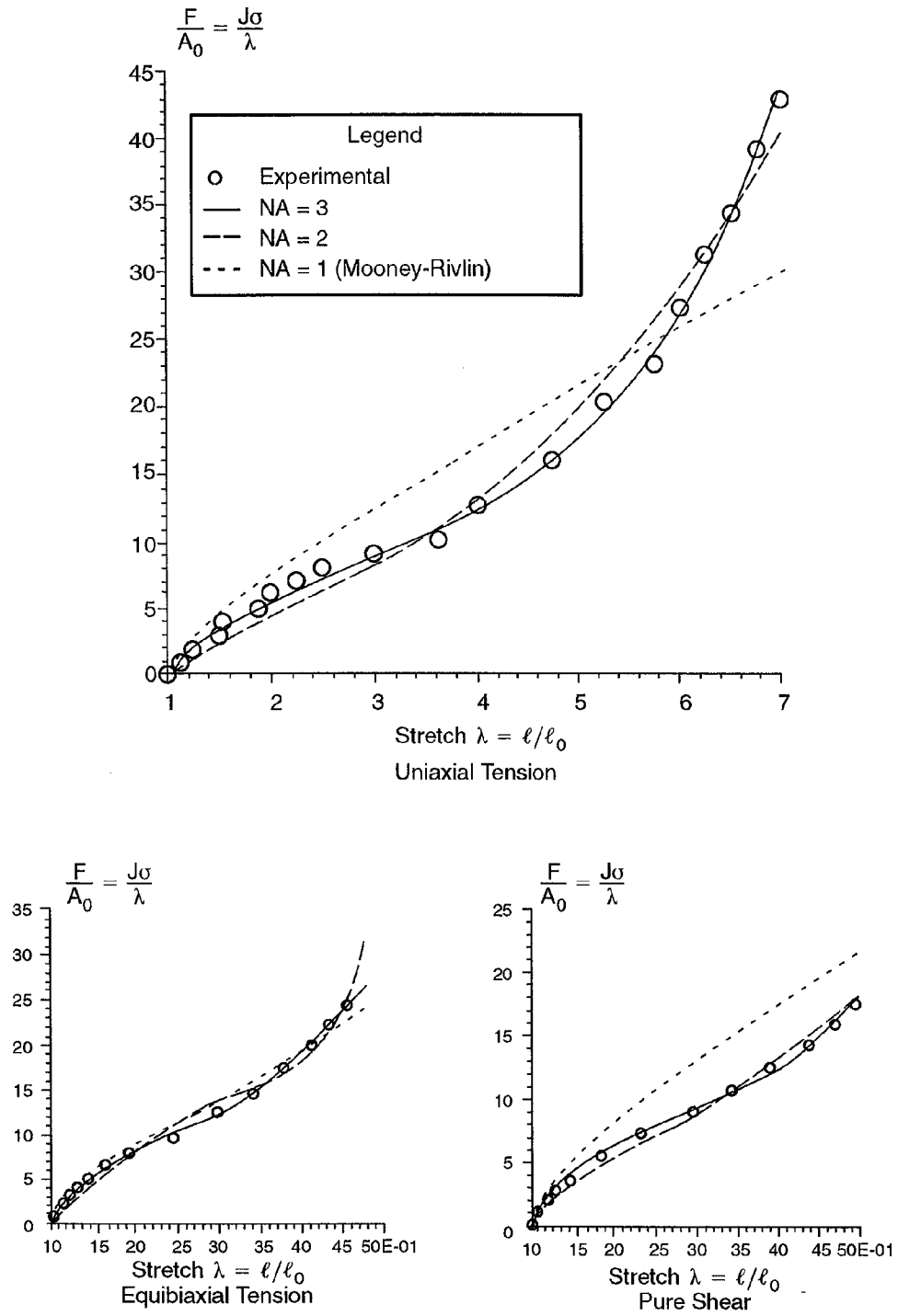


Figure 2. Homogeneous Tests for Hyperelastic Materials:
 Uniaxial Tension, Equibiaxial Tension, and Pure Shear.
 F =force, A_0 = original area, ℓ = current length, ℓ_0 = original length,
 $J = V/V_0$ (current volume / original volume).

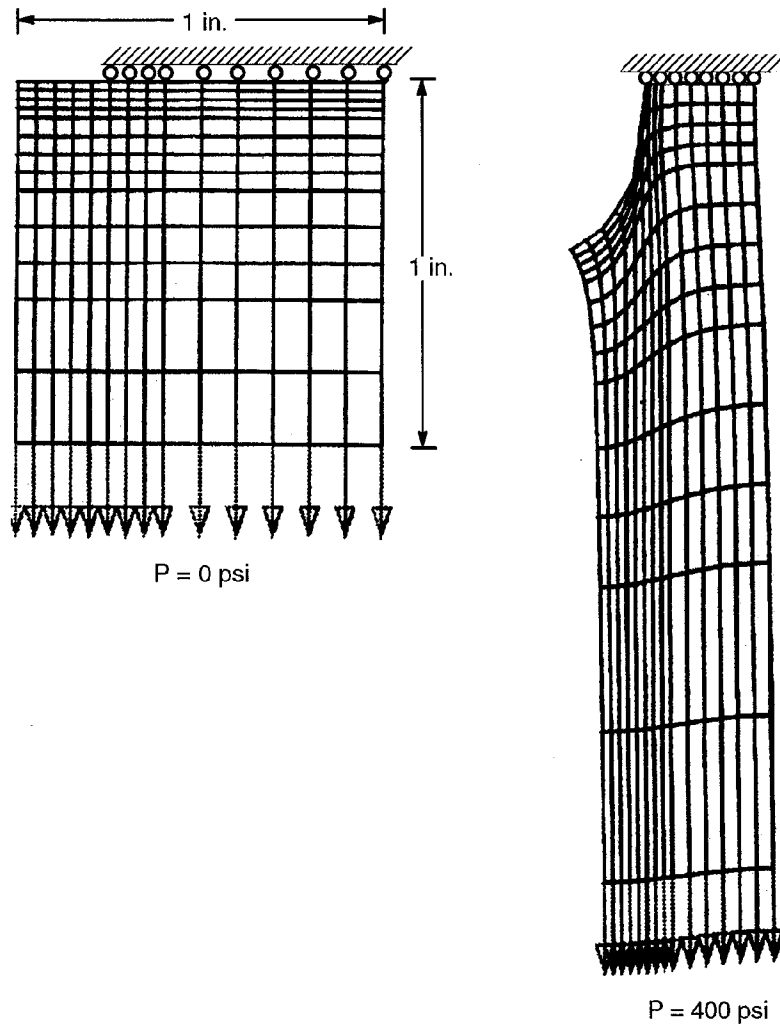


Figure 3. Stretching of a Rubber Rectangular Bar.

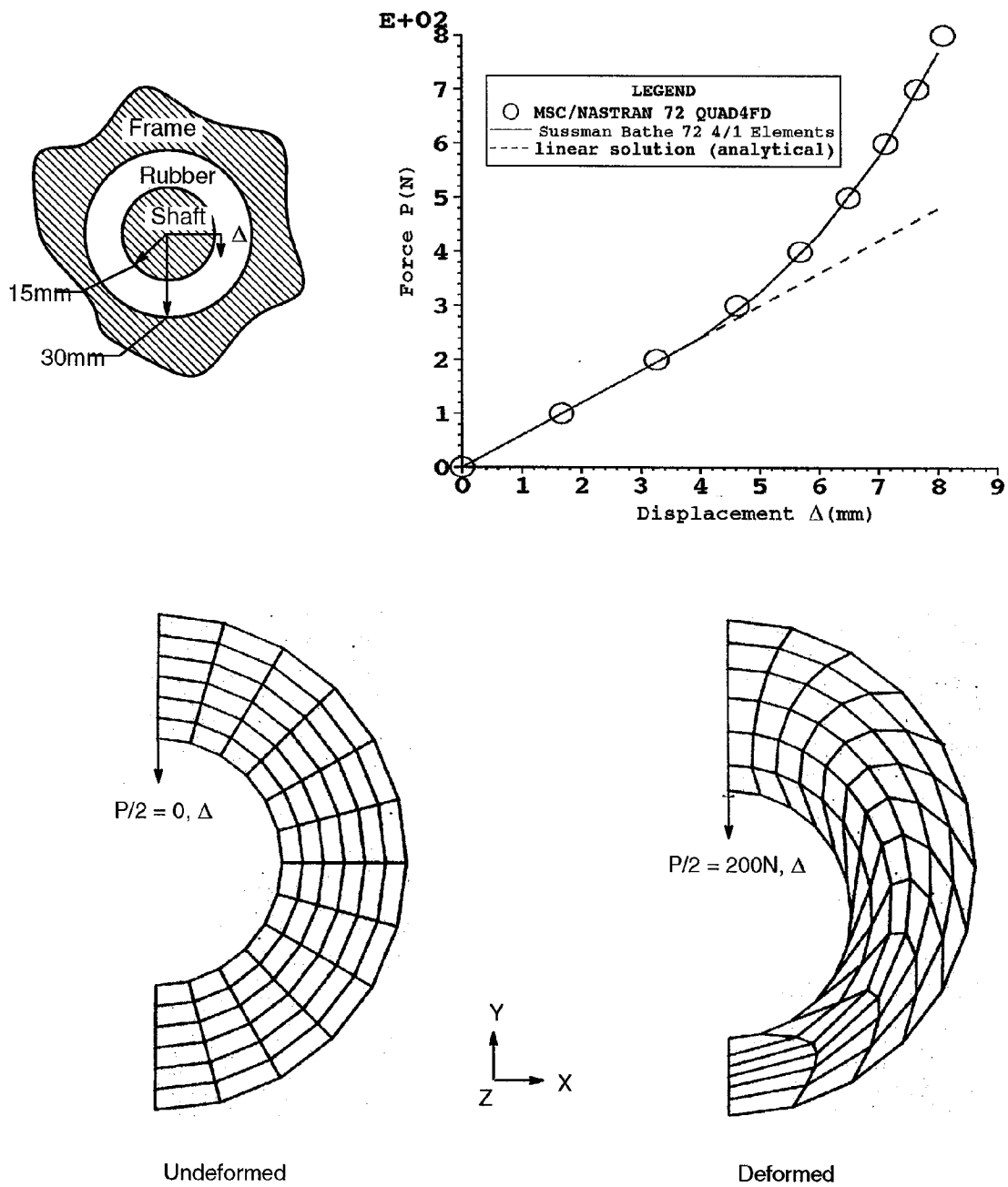
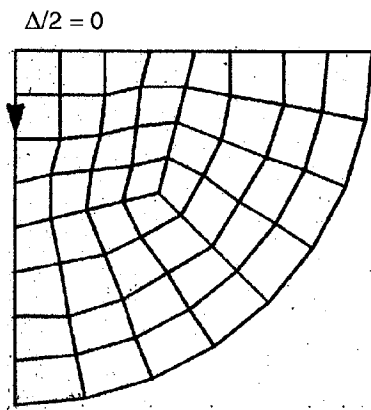
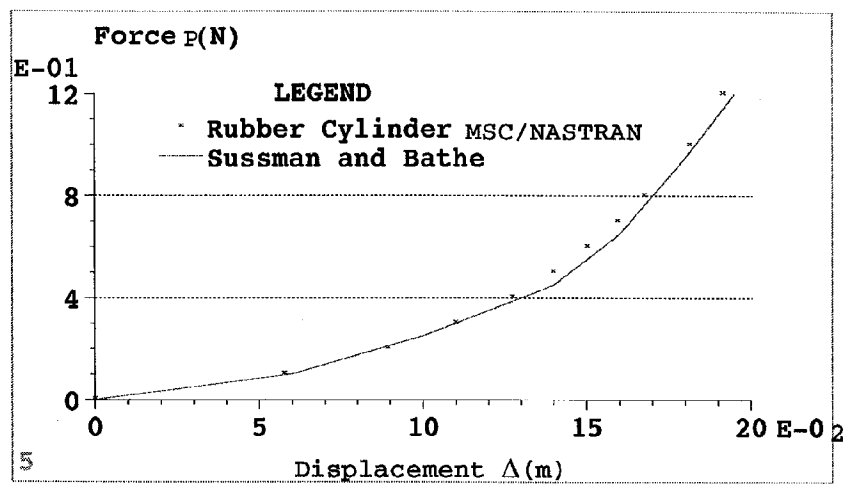
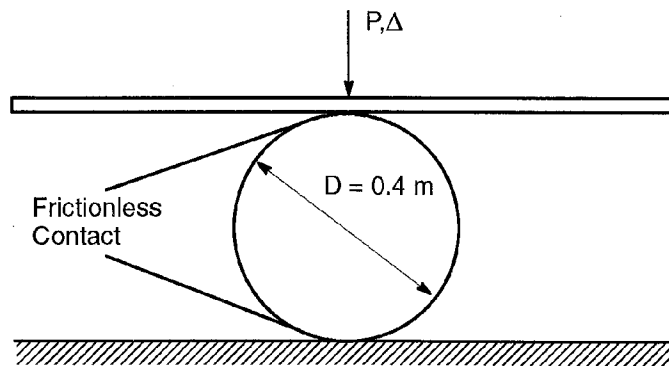
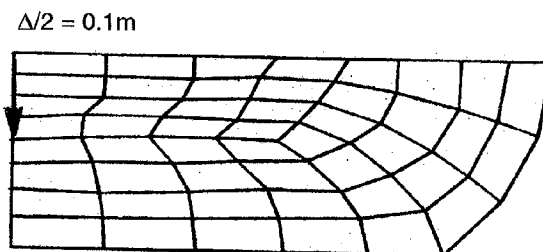


Figure 4. Rubber Bushing Problem.



Undeformed



Deformed

Figure 5. Lateral Compression of a Rubber Cylinder.